Available online www.jocpr.com

Journal of Chemical and Pharmaceutical Research, 2014, 6(3):1490-1495

Research Article

ISSN : 0975-7384
CODEN(USA) : JCPRC5

Electrochemical characterization of Ca_Sn metal composite oxides prepared by wet chemical route

Tao Liu[1], Rongbin Du[2]*, Xuejun Kong[1] and Junwei Wang[1]

[1]*School of Chemistry and Chemical Engineering, Anqing Normal College, Anqing, P R, China*
[2]*Anhui Key Laboratory of Functional Material, Anqing Normal College, Anqing, P R, China*

ABSTRACT

Crystalline $CaSnO_3 \cdot Ca_2SnO_4$ composite oxide was prepared by wet-chemical route and the electrochemical properties as anode material for lithium ion batteries were studied. The average size of crystal $CaSnO_3$ is 11.2nm and the average size of Ca_2SnO_4 is 9.6nm. The particle size of $CaSnO_3 \cdot Ca_2SnO_4$ composite oxide is 100-200 nm with aggregation in 750 ℃. But on the inside of the composite oxide, the sample breaks up to small particle about 33 nm. The reversible capacity of the sample is 678 mAh/g in the first cycle and the average decay of charge capacity is 1.37% per cycle after 20 cycles. The observed capacity involved in the first discharge and the reversible capacity during subsequent charge-discharge cycles shows that the electrochemical process in $CaSnO_3$ is similar to other Sn-based oxide materials, namely, an initial structural reduction with Sn-metal formation followed by reversible Li-Sn alloy formation.

Keywords: lithium ion batteries, Ca-Sn composite oxide, wet chemical route, anode

---

INTRODUCTION

Since YOSHIO et al[1] announced the commercialization of tin oxide as negative electrodes of 1ithium-ion batteries, the tin oxide anode has attracted much attention due to its high specific capacity, which is about twice that of graphite, and has been considered the best candidate for lithium-ion battery anode material[2−7]. When SnO_2 was used as the anode material of 1ithium- ion batteries, tin works as the virtual part, and its reversible capacity is based on the formation and decomposition of 1ithium tin alloys, LiSn, Li_7Sn_3, Li_5Sn_2, Li_3Sn_5, Li_7Sn_2 or $Li_{22}Sn_5$[8]. The oxygen in SnO_2 can combine with lithium to form Li_2O in the first cycle, which acts as the buffer for tin aggregation. Lithium intercalating in tin dioxide in the first cycle can be described by the following reactions[2 ,9, 10]:

$$4Li^+ + 4e^- + SnO_2 \rightarrow Sn + 2Li_2O, \quad (1)$$

$$xLi^+ + xe^- + Sn \underset{\text{charge}}{\overset{\text{discharge}}{\Leftrightarrow}} Li_xSn. \quad (2)$$

Different synthetic techniques can make SnO_2 with different particle sizes and morphologies, which can further affect its electrochemical performance[11,12]. Recently, alkaline earth metal Stannate $MSnO_3$(M=Mg，Ca，Sr，Ba) as a dielectric material, because of the thermal stability, its application in the capacitors are more concerned[11]. So far, dielectric properties, surface structure and microstructure of stannate are studied [13], but the research of calcium stannate as anode material in lithium-ion battery has not been reported in the literature. In this works, Crystalline $CaSnO_3 \cdot Ca_2SnO_4$ composite oxide was prepared by wet-chemical route and its electrochemical properties were investigated in detail.

EXPERIMENTAL SECTION

Preparation of samples $CaSnO_3 \cdot Ca_2SnO_4$

According to the literature [14], a equimolar amount of $CaCl_2$ and $SnCl_4$ was dissolved in de-ionized water to get a mixed aqueous solution, excess NaOH solution was added into the solution dropwise under continuous stirring, then continuously stirring for 5h, standing 15h, vacuum filtration, the resulting precipitate was washed with distilled water until neutral, then white powder was obtained by vacuum drying for 6 h at 80℃. Chemical reaction equation is:

$$Ca^{2+}+Sn^{4+}+6OH^- \rightarrow CaSn(OH)_6 \qquad (3)$$

The precursor $CaSn(OH)_6$ was calcined at 750℃ to obtain the product of $CaSnO_3 \cdot Ca_2SnO_4$.

Material characterization

The phase of the samples was characterized by X-ray diffraction(XRD, Rigaku D/MAX-gA) with a mono-chromatic Cu Kα radiation (0.15405 nm). The thermal behavior of the precursor was investigated by thermogravimetric analysis(TGA) and differential thermal analysis(DTA) on a TGA-SDTA851 ethermal analysis system(Mettler Toledo Corp) from room temperature(25℃) to 600℃ in Ar atmosphere at a heating rate of 10℃/min. TEM was performed on a JEOL-2010 transmission electron microscope with an accelerating voltage of 200 kV. The grain size was calculated using the Scherrer formula of $D=0.89\lambda/\beta\sin\theta$, in which D is the crystalline size, λ is the wavelength of X-ray, and θ is the diffraction peak angle.

Electrode preparation and electrochemical characterization

A certain amount of $CaSnO_3 \cdot Ca_2SnO_4$, acetylene black and polyvinylidene difluoride(PVDF) was made into slurry with a mass ratio of 70:20:10 in N-methyl pyrolidinone(NMP). The mixture was then coated on copper foils followed by a drying in vacuum at 120℃ for 10 h to obtain the study electrode. The electrochemical tests were conducted using a conventional coin-type(2025) cell, employing $CaSnO_3 \cdot Ca_2SnO_4$ as positive electrode, a polypropylene microporous separator, utilizing 1.0 mol/L $LiPF_6$ in ethylene carbonate/dimethyl carbonate (EC/DMC) (with an EC to DMC volume ratio of 1:1) as the electrolyte and lithium foil as negative electrode. The assembly was carried out in an Ar-filled glove box. The discharge-charge tests were done with a PCBT-110-8D battery tester under a constant current rate of 0.2C and a constant temperature of (25±0.01)℃ in the voltage range of 0−2.0V. Here, the discharge process means the process of Li^+ insertion into $CaSnO_3 \cdot Ca_2SnO_4$ electrode and the charge process means the process of Li^+ deinsertion out of $CaSnO_3 \cdot Ca_2SnO_4$electrode.

RESULTS AND DISCUSSION

The X-ray diffraction (XRD) pattern of the sample was shown in Fig.1. All the diffraction peaks were consistent well with the pure cubic phase $CaSn(OH)_6$ (JCPDS No.09-0030), and there were no extra peaks in the pattern. Obviously, $CaSn(OH)_6$ without impurity was successfully synthesized by this wet-chemical method. The narrow and sharp diffraction peaks implied high crystallinity of the sample.

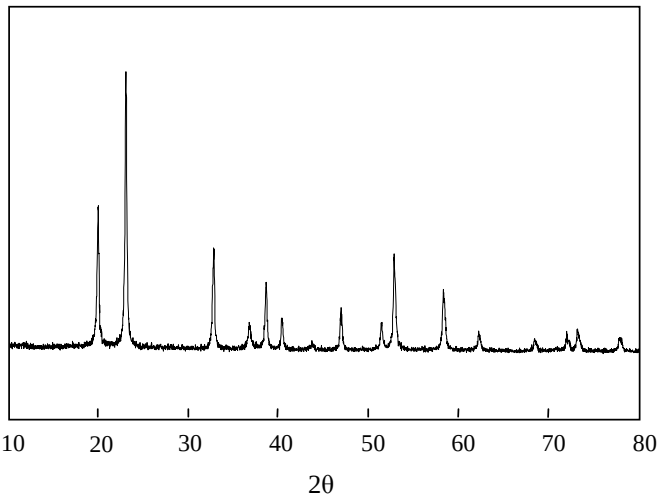

Fig.1 XRD patterns of precursor $CaSn(OH)_6$

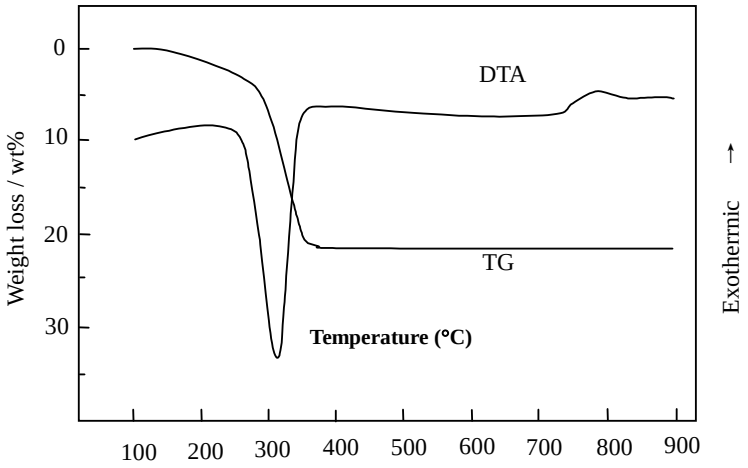

Fig. 2 DTA and TG curves of $CaSn(OH)_6$ in air

Fig.2 shows the TG-DTA curves of the precursor. From TG curve, the precursor loses its mass at about 150℃, which is assigned to be the evaporation of physically absorbed water. At about 270℃, the precursor begins to decompose and lose water until almost all water is lost at about 350℃(mass loss 20.82%) with the formation of $CaSnO_3$, which basically agrees with the theoretical value (20.77%). From DTA curve, a n obvious endothermic peak at 310℃ appears, which can be attributed to the decomposition of $CuSn(OH)_6$ with the loss of water molecules. A small exothermic peak at between 720℃ and 820℃ is due to the further crystallization and reaction of $CaSnO_3$.

Pattern of as-product after thermal treatment of precursor at 750°C for 3h is displayed in Fig.3. Chemical composition of the anode material has changed, the diffraction peaks of $CaSn(OH)_6$ disappear, and some diffraction peaks of other substances appear, which are the characteristic peaks of $CaSnO_3$（JCPDS 31-0312）and Ca_2SnO_4（JCPDS 23-0723）. The crystallite size of the sample was also estimated by the Scherrer's equation. The average size of the nanoparticles $CaSnO_3$ is calculated to be about 27.8 nm, the average size of the nanoparticles Ca_2SnO_4 9.6nm.

TEM image of the products $CaSnO_3$ obtained after thermal treatment of precursor at 600°C is shown in Fig.4, Which indicates that these particals have a square shape and good dispersity, the average particle size is in the range of 80-150 nm.

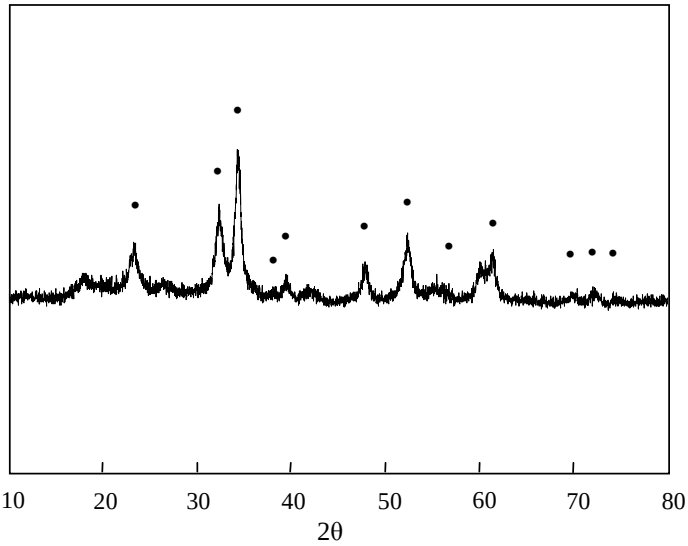

Fig. 3 XRD patterns for $CaSnO_3 \cdot Ca_2SnO_4$
$CaSnO_3$ peaks are marked with " ●" , the remaining peaks belong to Ca_2SnO_4.

Fig. 5 shows the TEM images of the $CaSnO_3 \cdot Ca_2SnO_4$ powder obtained from calcining the $CaSn(OH)_6$ precursors at 750℃. Compared with Fig.4, at 750℃, many particles agglomerate into larger particles about the size of 100-200nm, but internally they break up to smaller particles about the size of 33nm. Sample structure, changes in the

composition and particle size will inevitably lead to changes in their electrochemical properties.

The initial two discharge-charge curves of $CaSnO_3 \cdot Ca_2SnO_4$ anode are shown in Fig.5. In the first discharge curve, the potential rapidly drops to reach a plateau at 0.8V, then slowly decreases down to 0V, plateau can be observed at about 0.6V in the first charge curve, which is similar to most tin-based oxide cathode[15], the first discharge process corresponding to the lattice destruction and tin generation, reaction equation is:

$CaSnO_3 + 4Li^+ + 4e^- \rightarrow CaO + 2Li_2O + Sn$ (4)

$Ca_2SnO_4 + 4Li^+ + 4e^- \rightarrow 2CaO + 2Li_2O + Sn$ (5)

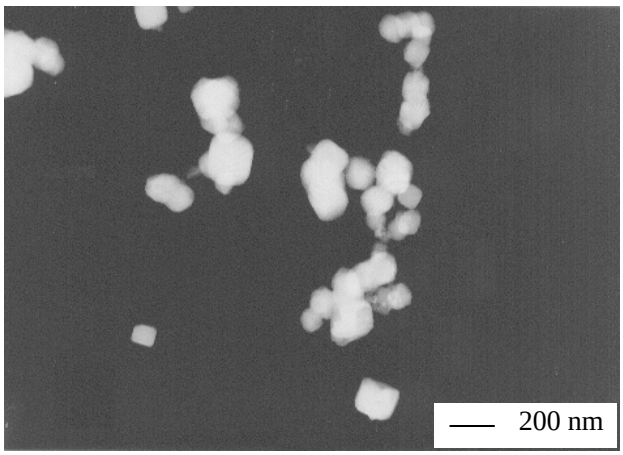

Fig. 4 TEM image of $CaSnO_3$ prepared at 600℃

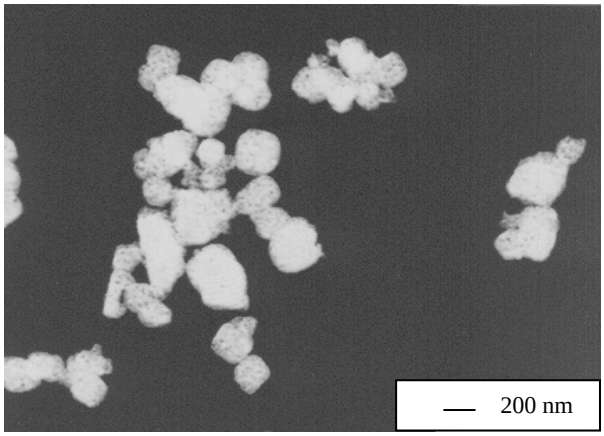

Fig. 5 TEM image of $CaSnO_3 \cdot Ca_2SnO_4$ prepared at 750℃

Then, during the cycle, chemical reaction formula(2). In the charge curves, The discharge capacity of $CaSnO_3 \cdot Ca_2SnO_4$ electrode in the first discharge reaches 1618 mA·h/g, equivalent to 12.4 lithium consumption, which is more than the theoretical value 8.4 by reaction (4), (5) and (2), which may be related to more reaction interface formation because of adding more conductive carbon in the electrode preparation process. The first charge capacity amounts to 678mAh/g, the first-cycle irreversible loss is 58.1%. Reaction (3), (4) the reaction is irreversible, which corresponds to the irreversible capacity loss. According to the reaction formula (3), (4) , the calculated $CaSnO_3 \cdot Ca_2SnO_4$ irreversible capacity loss is 561 mAh/g. Since in the first discharge process, a layer of inert surface film forms at the electrode / solution interface, leading to large irreversible capacity loss. Reaction (2) is a reversible reaction, corresponding to the reversible capacity in charge and discharge。

Fig.7 shows the variation of reversible capacity as a function of cycle number. For $CaSnO_3 \cdot Ca_2SnO_4$, during the first week of the cycle, there is a large irreversible capacity loss. From the second week, the charge-discharge efficiency obtains more than 90%. this material shows moderate capacity fading with cycling, which may result from the lithium loss because of easy decomposition of the electrolyte with the help of $CaSnO_3 \cdot Ca_2SnO_4$ as catalyst. In the 20th cycle, the charge capacity is 491 mAh/g, the average capacity fade rate is 1.37% per cycle.

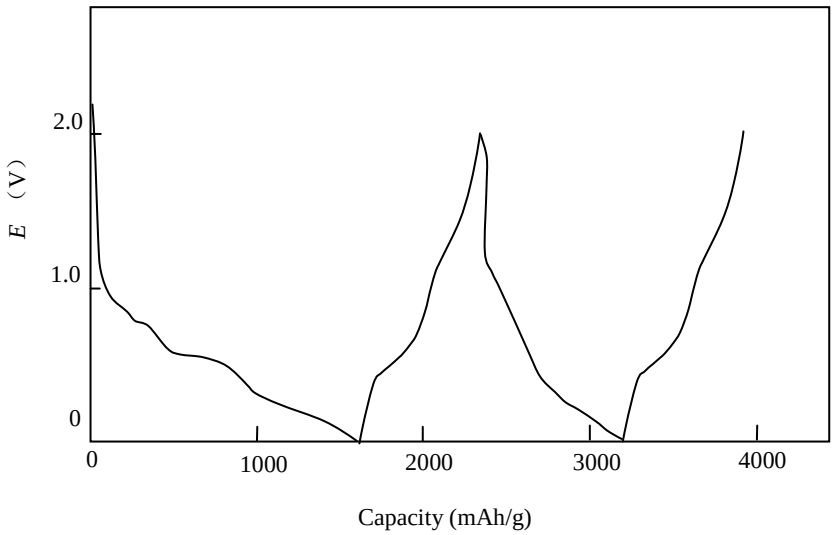

Fig. 6 The first two discharge-charge curves of $CaSnO_3 \cdot Ca_2SnO_4$ anode

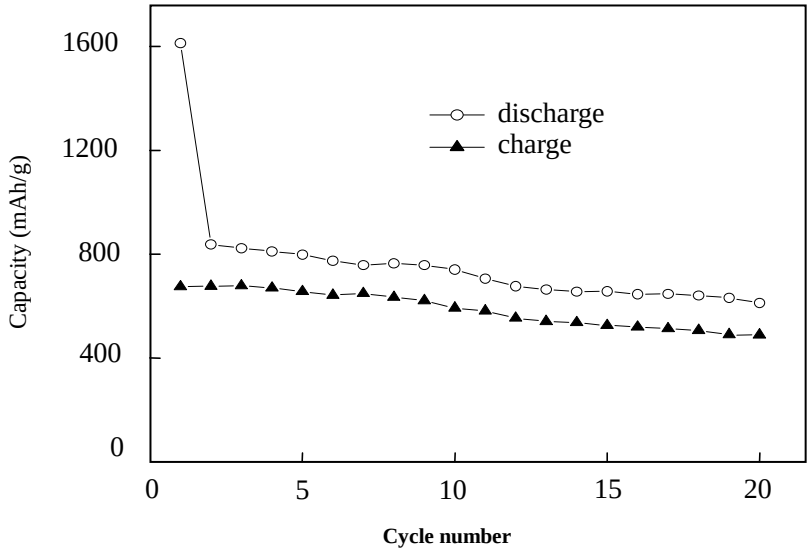

Fig. 7 Cycle- ability of $CaSnO_3 \cdot Ca_2SnO_4$ anode

CONCLUSION

By wet-chemical route using $SnCl_4$,$CaCl_2$ and NaOH as raw materials, Crystalline $CaSnO_3 \cdot Ca_2SnO_4$ composite oxide was prepared as a novel anode material for lithium ion batteries. The average size of crystal $CaSnO_3$ is 11.2nm and the average size of Ca_2SnO_4 is 9.6nm. The particle size of $CaSnO_3 \cdot Ca_2SnO_4$ composite oxide is 100-200 nm with aggregation in 750℃. But on the inside of the composite oxide, the sample breaks up to small particle about 33 nm. $CaSnO_3 \cdot Ca_2SnO_4$ has the similar lithium storage mechanism with other Tin-based oxides.The initial capacity during the first lithium insertion is 1618 mAh/g. The reversible capacity of the sample is 678 mAh/g in the first cycle and the average decay of charge capacity is 1.37% per cycle after 20 cycles, which indicats the presence of calcium ions may improve the performance of tin-based anode materials.Further work is needed to fully study the mechanism, to improve the cycle life, and to make it a commercially available material.

Acknowledgement
This work was supported by The National Natural Science Foundation of China (20706001), the Natural Science Foundation of Anhui Province (070414164), and Project under Scientific and Technological Planning of Education Office of Anhui Province (KJ2009B108).

REFERENCES

[1] I Yoshio, K Tadahiko, *Science*, **1997**, 27(6), l395−1397.

[2] IA Courtney, JR Dahn, *J.Electrochem Soc*., **1997**, 144(6), 2045−2052.
[3]MS Tihile, PA Murade, *J.Chem. Pharm. Res.*, **2013**, 5(2),5-9.
[4] GX Wang, J Yao, HK Liu, *Electrochem Solid-State Lett*, **2004**, 7(8), 250−253.
[5] J Payamara, A Payamara, *J.Chem. Pharm. Res.*, **2009**, 1(1),187-190.
[6] KD Kepler, JT Vaughey, MM Thackeray, *Electrochem Solid-State Lett*, **1999**, 2(5),307−309.
[7] S Chandra, D Jain, B Ratnam, *J.Chem. Pharm. Res.*, **2010**, 2(1): 533-538.
[8] LY Beaulieu, JR Dahn, *J.Electrochem Soc.*, **2000**, 147(8), 3 237−3 241.
[9] M Mustapha, B R Thorat, S Sawant, R G Atram, *J.Chem. Pharm. Res.*, **2011**, 3(4): 533-538.
[10] T Brousse, R Retoux, U Herterich, *J.Electrochem Soc*., **1998**, 145(1),1−4.
[11] O Mao, JR Dahn. *J.Electrochem Soc.*, **1999**, 146(2), 414−422.
[12] C Srinivas, V Bhushanam, TP Sagar, C Nagamani, M Rajasekhar, *J.Chem. Pharm. Res.*, **2010**, 2(5),10-15.
[13] GM Eehrlich, C Durand, X Chen. *J.Electrochem Soc*.,**2000**, 147(2), 886−891.
[14] J Yang, M Winter, JO Besenhard. *Solid State Ionics*, **1996**, 90(1-4), 281−287.
[15] M Wachtler, MR Wagner, M Schmied. *J Eeltroanal Chem.*, **2001**, 510(1-2),12−19.